

Weakly Supervised Grounding for VQA in Vision-Language Transformers

Aisha Urooj Khan¹[0000–0001–6521–2512], Hilde Kuehne^{2,3}[0000–0003–1079–4441],
Chuang Gan³[0000–0003–4031–5886], Niels Da Vitoria Lobo¹[0000–0001–5354–2805],
and Mubarak Shah¹[0000–0001–6172–5572]

¹ University of Central Florida, Orlando, FL, USA

² Goethe University Frankfurt, Frankfurt, Hesse, Germany

³ MIT-IBM Watson AI Lab, Cambridge, MA, USA

Abstract. Transformers for visual-language representation learning have been getting a lot of interest and shown tremendous performance on visual question answering (VQA) and grounding. But most systems that show good performance of those tasks still rely on pre-trained object detectors during training, which limits their applicability to the object classes available for those detectors. To mitigate this limitation, the following paper focuses on the problem of weakly supervised grounding in context of visual question answering in transformers. The approach leverages capsules by grouping each visual token in the visual encoder and uses activations from language self-attention layers as a text-guided selection module to mask those capsules before they are forwarded to the next layer. We evaluate our approach on the challenging GQA as well as VQA-HAT dataset for VQA grounding. Our experiments show that: while removing the information of masked objects from standard transformer architectures leads to a significant drop in performance, the integration of capsules significantly improves the grounding ability of such systems and provides new state-of-the-art results compared to other approaches in the field⁴.

Keywords: visual grounding, visual question answering, vision and language

1 Introduction

Enabling VQA systems to be explainable can be important for variety of applications such as assisting visually-impaired people to navigate [17, 67] or helping radiologists in early diagnosis of fatal diseases [1, 68]. A system that only produces a good answering accuracy will not be sufficient in these applications. Instead, VQA systems for such uses should ideally also provide an answer verification mechanism and grounding is a convincing way to obtain this direct verification.

⁴ Code will be available at <https://github.com/aurooj/WSG-VQA-VLTransformers>

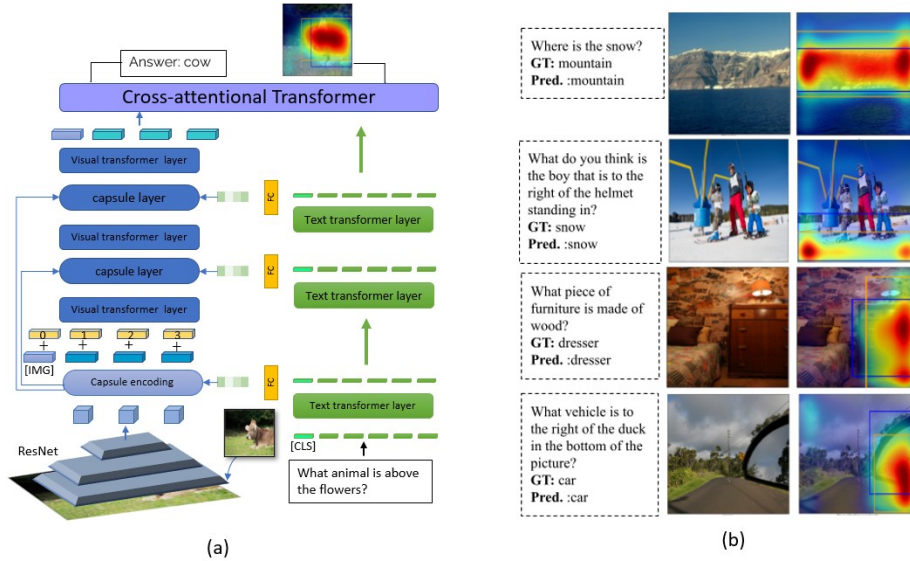


Fig. 1: (a) **Proposed architecture**: Given the question-image pair, grid features are used to obtain visual capsules using a Capsule encoding layer. Output embedding for [CLS] token from text transformer layer is then used to do capsule features selection. Selected capsules encodings with position information is then input to the visual encoder. We use sentence embedding from each textual transformer layer to select capsules for each visual transformer layer. The selected capsules are then input to the next visual transformer layer along with the output of the previous layer in the visual encoder. Finally, a cross-attentional block allows for a fine-grained interaction between both modalities to predict the answer. (b) **Attention from the proposed vision-language transformer with VQA supervision**. We look at the self-attention of the [IMG] token on the heads of the last layer. These maps show that the model automatically learns to ground relevant objects leading to weakly-supervised grounded VQA (GVQA). blue box is ground truth, orange is predicted box.

Following upon success in natural language processing and multi-modal understanding, a variety of transformer-based methods have been introduced for joint representation learning of vision and language and respective downstream tasks, including VQA. Such approaches, e.g., [37, 43, 60] are usually trained based on region masks of detected objects generated by a pre-trained object detector [29]. The assumption that object masks are provided at input time limits detection to pretrained objects only and comes at the risk of image context information being lost.

Detector-free methods avoid this bias toward pre-trained object classes while being simpler and faster because they do not need to extract region-based features from a pre-trained object detector. Other works [10, 24, 31, 52] have therefore focused on removing the dependency on object detectors while achieving comparable if not better performance (e.g., on retrieval and VQA tasks). Among

those, [10] and [52] also show good visual representations by qualitative examples, but do not provide an evaluation of their answer (or question) grounding ability.

In this work, we want to address this issue and focus on the problem of weakly supervised grounding for the VQA task in visual-language transformer based systems. Compared to detector-free referential expression grounding [7, 41, 64], VQA breaks the assumption that the region description is always part of the input phrase as the answer word may not be present in the input question. It is therefore not enough to only learn a direct mapping between text and image features, but also requires processing multiple image-text mapping steps with the correct relation between them.

To address the task of VQA grounding in transformer-based architectures with the question-answering supervision alone, we propose a generic extension of the visual encoder part of a visual-language transformer based on visual capsule layers together with a text-guided selection module. Capsule networks learn to group neurons into visual entities. They thus try to capture entities (objectness) and relationships among them with promising results on various visual detection and segmentation tasks [13, 14, 34]. To make use of this ability in context of transformers, we transfer inputs as well as intermediate layers’ feature tokens to capsule encodings, from which the most relevant ones will be selected by the textual tokens of a parallel language encoder. We propose to interleave transformer layers with such masked residual capsule encodings. This extension provides a combination of visual input routing and text-based masking which significantly improves the visual grounding ability of such systems.

We evaluate existing methods as well as the proposed approach on the challenging GQA and VQA-HAT datasets. To this end, we consider the attention output obtained from these methods and evaluate it on various metrics, namely overlap, intersection over union, and pointing game accuracy. Our results on the original architectures show a significant gap between task accuracy and grounding of existing methods indicating that existing vision-language systems are far from learning an actually grounded representation. The proposed method bridges the gap and outperforms the best contenders in terms of overlap, intersection over union, and pointing game accuracy achieving SOTA performance on the GQA dataset. It also achieves best performance (in terms of mean-rank correlation score) on VQA-HAT [8] dataset among methods which do not use attention supervision.

We summarize contributions of our architecture as follows: a) we propose a capsule encoding layer to generate capsule-based visual tokens for transformers; b) we propose a text-guided capsule selection with residual connections to guide the visual features at each encoding step; and c) we propose generic interleaved processing that can be integrated in various vision language architectures.

2 Related Work

Visual-language Representation Learning. Learning a robust visual-language representation is currently an active area of research [30] with impressive progress

on downstream tasks including VQA [6, 35, 37, 38, 42, 43, 46, 59, 60]. A majority of these methods rely on object detections making the downstream task simpler. Some works have attempted to avoid this dependency on object detections and show comparable performance using spatial features or image patches [23, 24, 31, 36]. Our work also falls into the later category and uses grid features as input.

Weakly-supervised Grounding and VQA. Weakly-supervised visual grounding is well studied for phrase-grounding in images [3, 5, 7, 9, 41, 61, 64]. Few works also focused on phrase grounding in videos [22, 58, 65]. However, less attention has been paid to the VQA grounding despite having significance for many critical applications. There are many works on making questions visually grounded [48, 53, 57, 62, 70, 71], but only a handful of works are focused to evaluate their grounding abilities [8, 26, 28, 51, 55, 57]. GQA leverages scene graphs from Visual Genome dataset providing visual grounding labels for question and answer making it feasible to evaluate VQA logic grounding. Recently, xGQA [49] has been introduced as a multilingual version of GQA benchmark. GQA [26] and [28] discuss the evaluation of VQA systems for grounding ability. VQA-HAT [8] on the other hand, provides human attention maps used for answering the question in a game-inspired attention-annotation setup. A handful of methods [44, 51, 66] evaluate their systems for correlation between machine-generated attention and human attention maps on VQA-HAT. However, with the emergence of transformers as the current SOTA, the focus moves towards grounding abilities of those systems for VQA task. Unfortunately, none of these transformer-based methods have yet focused on the evaluation of weakly supervised grounding. However, the fact that only few real-world dataset provide grounding labels makes this task challenging. We therefore finetune three existing detector-free transformer methods on GQA and evaluate them for the weak grounding task.

Transformers with Capsules. There are few works who focused on the idea of combining transformers and capsules [12, 16, 40, 45, 47, 50, 63]. For instance, [63] studies text-summarization, image-processing, and 3D vision tasks; [47, 50] uses capsule-transformer architecture for image-classification, and [40] uses capsules-transformers for stock movements prediction. To the best of our knowledge, no one has studied the combination of capsules with transformers for VQA grounding.

3 Proposed Approach

Given an input image-question pair with image I and question Q , we want to localize the relevant question and answer objects with only VQA supervision. We start from a two stream visual-language model where the language encoder L_e guides input and intermediate representations of the visual encoder V_e . The input text to the language encoder L_e is a sequence of word tokens from a vocabulary V appended with special tokens $[CLS]$ and $[SEP]$ at the start and end of the word tokens. As input to the visual encoder, our model takes convolutional features as image embeddings. The convolutional features $X \in \mathbb{R}^{h \times w \times d1}$ are extracted from a pre-trained ResNet model, h, w are the feature height and width, and $d1$ is the

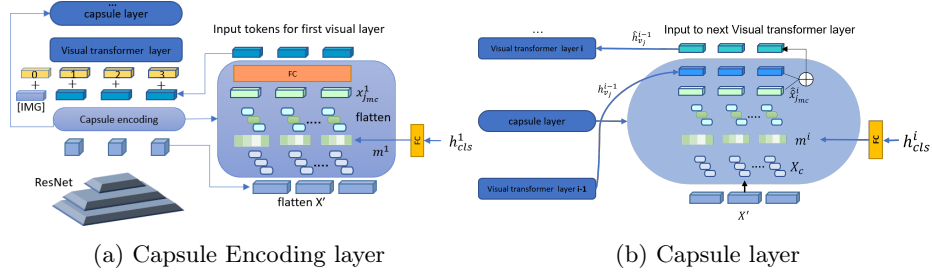


Fig. 2: **(a) Capsule encoding layer:** grid features $X' \in \mathbb{R}^{h \times w \times d}$ are transformed into capsules X_c for each spatial position. Output embedding h_{cls}^1 for $[CLS]$ token from the first text encoder layer generates a mask m^1 for capsule selection. The selected capsules X_{mc}^1 are flattened along capsule dimension to get a set of visual tokens (of length $h * w$) where each token is denoted by $x_{jmc}^1, j = \{1, 2, \dots, hw\}$; $x_{jmc}^1 \in \mathbb{R}^{d_c}$ where d_c =capsule dimension, is then upsampled to model dimension d using a fully connected layer. A position embedding is added to visual tokens with the special token $[IMG]$ at position 0. The output capsule encodings are then input to the visual transformer for future steps. **(b) Capsule layer:** Similar to the Capsule encoding, input tokens X' are first transformed into capsules X_c . The output feature h_{cls}^i corresponding to $[CLS]$ token from the text encoder layer i learns the presence probability of a certain capsule at the layer i in visual encoder. This mask m^i selects the capsules respective to the attended words at text encoder layer i . The resulting capsules are then flattened and upsampled (denoted by \hat{x}_{jmc}^i) and added to the output h_{cls}^{i-1} of the previous visual transformer layer $i - 1$ to obtain input features $\hat{h}_{v_j}^{i-1}$ for the next visual transformer layer i .

extracted features dimension. A 2D convolutional layer then yields an embedding X' of size $\mathbb{R}^{h \times w \times d}$, where d is the model dimension size. These input embeddings are used to produce capsule encodings X_c as explained in section 3.2.

In the following, we first explain the motivation to use capsules in Sec. 3.1 followed by details about the capsule encoding in Sec. 3.2, the text-guided selection of the capsules in Sec. 3.3, as well as the text-based residual connection in Sec. 3.4. We close the section with an overview of the pretraining procedure in Sec. 3.5 and describe the details of the VQA downstream task in Sec. 4.1.

3.1 Capsule Networks

Convincing amount of evidence exist in psychology that humans parse visual scenes into part-whole hierarchies by modelling the viewpoint-invariant spatial relationship between a part and a whole [18, 27]. Neural Networks can profit from understanding images in the same way humans do to become more transparent and interpretable. However, standard NNs lack this ability to dynamically represent a distinct part-whole hierarchy tree structure for each image [19].

This inability motivated the introduction of a type of model called Capsule Networks [20] which was later formalized in [56]. A Capsule Network is a neural network that is designed to model part-whole hierarchical relationships more explicitly than Convolutional Neural Networks (CNNs), by using groups of neurons to encode entities and learning the relationships between these entities.

The promising performance of capsules can be attributed to their ability to learn part-whole relationships for object entities via routing-by-agreement [56] between different capsule layers. A capsule is represented by a group of neurons; each capsule layer is comprised of multiple capsules and multiple capsules layers can be stacked together. Capsule routing is a non-linear, iterative and clustering-like process that occurs between adjacent capsule layers, dynamically assigning *part* capsules i in layer ℓ to *object* capsules j in layer $\ell + 1$, by iteratively calibrating the routing coefficients γ [54]. Unlike most previous works which use a loss over object classes to learn a set of capsule classes, we do not have any object level supervision available for capsules, but instead combine the power of transformers and capsules by interleaving capsules as intermediate layers within the transformer and use VQA supervision to model visual entities as capsules.

3.2 Capsule Encodings

We use matrix capsules [21] as follows: given an image embedding $X' \in \mathbb{R}^{h \times w \times d}$, matrix capsules $X_c \in \mathbb{R}^{h \times w \times d_c}$, as shown in Figure 2(a), are obtained as follows: The image embedding X' is input to a convolutional layer producing primary capsules X_p where each capsule has a pose matrix of size $K \times K$ and an activation weight. The primary capsule layer outputs C_p number of capsules for each spatial location. The output dimensions for poses is $\mathbb{R}^{h \times w \times C_p \times K \times K}$ and for activation is $\mathbb{R}^{h \times w \times C_p \times 1}$. To treat each capsule as a separate entity, the pose matrix and activation is grouped together for each capsule. Hence, the primary capsules X_p have the dimensions $\mathbb{R}^{h \times w \times d_p}$ where $d_p = C_p \times (K \times K + 1)$. The primary capsules are then passed through an EM-Routing layer to vote for capsules in the next layer. Assuming we have C_v number of capsules in the next layer, the routing yields capsule encodings X_c where $X_c \in \mathbb{R}^{h \times w \times d_c}$, $d_c = C_v \times (K \times K + 1)$. We use an equal number of capsules in both layers i.e., $C = C_p = C_v$. Our system employs the capsule representation X_c as visual embeddings.

Since transformers take a sequence of tokens as input, we flatten the capsule embeddings across spatial dimension to get a sequence of visual tokens of length $h \times w$, where each visual token is denoted by $x_j \in \mathbb{R}^{d_c}$ for $j \in 1, 2, \dots, hw$. A special trainable token $[IMG]$ is then concatenated to these tokens to form the final set of visual tokens $\{[IMG], x_1, x_2, \dots, x_{hw}\}$. A learnable position embedding is added to these visual tokens to keep the notion of spatial position in the sequence. Each of the visual tokens except $[IMG]$ is represented by C capsules.

3.3 Text-guided Capsule Selection

As the language encoder is attending different words at each layer, we select visual capsules based on the text representation at each visual encoder layer. Let h_{cls}^i be the feature output corresponding to $[CLS]$ token from the i^{th} text encoder layer; we take the feature output h_{cls}^1 against $[CLS]$ token from first text encoder layer and input to a fully connected layer ϕ . The output is C logits followed by a softmax function to learn presence probability $m^1 \in \mathbb{R}^C$ of attended

words at layer 1. This mask is applied to X_c to select the respective capsules and mask out the rest resulting in the masked capsule representation X_{mc}^1 .

$$m^1 = \text{softmax}(\phi(h_{cls}^1)). \quad (1)$$

$$X_{mc}^1 = m^1 \odot X_c \quad (2)$$

The masking is only applied to the visual tokens x_j without affecting $[IMG]$ token.

3.4 Text-based Residual Connection

To keep the capsule representation between intermediate layers, we add capsules via a residual connection to the inputs of each intermediate visual encoder layer. The input capsules to the intermediate layer are also selected based on the intermediate features output from text encoder. Let m^i be the probability mask for attended words in the text feature output h_{cls}^i from the i^{th} layer:

$$m^i = \text{softmax}(\phi(h_{cls}^i)), \forall i \in \{1, 2, \dots, L\}, \quad (3)$$

and $x_{j_{mc}}^i$ denotes the j^{th} token with visual capsules selected using mask m^i .

$$x_{j_{mc}}^i = m^i \odot X_c, \quad (4)$$

The i^{th} visual encoder layer takes features from $(i-1)^{th}$ layer to produce features $h_{v_j}^i$ for j^{th} position. Let f_v^i be the i^{th} layer in the visual encoder. The output and input follow the notation below:

$$h_{v_j}^i = f_v^i(h_{v_j}^{i-1}). \quad (5)$$

To keep reasoning flowing from text to image, we propose to add the residual connection from visual capsules for j^{th} token by adding $x_{j_{mc}}^i$ to the input of i^{th} encoder layer. However, there is a dimension mismatch between $x_{j_{mc}}^i \in \mathbb{R}^{d_c}$ and $h_{v_j}^{i-1} \in \mathbb{R}^d$. We upsample $x_{j_{mc}}^i$ to dimension size d using a fully connected layer σ and get the upsampled capsule-based features $\hat{x}_{j_{mc}}^i \in \mathbb{R}^d$. The input to the visual encoder layer will be as follows:

$$\hat{h}_{v_j}^{i-1} = f_v^i(h_{v_j}^{i-1} + \hat{x}_{j_{mc}}^i). \quad (6)$$

The output feature sequences from both encoders are then input to our cross attentional module which allows token-level attention between the two modalities. The aggregated feature outputs corresponding to $[CLS]$ and $[IMG]$ tokens after cross attention are input to a feature pooling layer followed by respective classifiers for pretraining and downstream tasks. We discuss the implementation about modality-specific encoders, feature pooling, and cross attention in detail in the supplementary.

3.5 Training

To perform well, transformers require pretraining on large-scale datasets before finetuning for the downstream tasks, i.e., GQA and VQA-HAT in our case. Therefore, we first pretrain our capsules-transformer backbone on three pretraining tasks: image-text matching (ITM), masked language modeling (MLM), and visual question answering (VQA). The system is pre-trained in two stages: first, we do joint training of modality-specific encoders only to learn text-guided capsules representation; the representation learned in encoders is kept fixed during the second stage of pre-training where we add cross-attentional blocks on top of the modality encoders allowing token-level interaction between text features and visual features. While the first stage of pretraining uses pooled features from text and from visual encoders, the second stage pools features after cross attention: therefore, the second stage pre-training tasks uses cross-modal inputs as language and image features. For details about pretraining tasks in context of our method, refer to section 1.2 in supplementary. We finally finetune the pretrained capsules-transformer backbone to solve VQA as our downstream task.

4 Experiments and Results

4.1 Datasets

Pre-training. We use MSCOCO [39] and Visual Genome [33] for pretraining our backbone. We use the same data as [60] which also include MSCOCO-based VQA datasets: Visual7W, VQAv2.0, and GQA. However, we exclude the GQA validation set from pretraining and finetuning as we evaluate grounding on this set (scene graphs for GQA test and testdev are not publicly available). We use train sets of MSCOCO and VG with ~ 7.5 M sentence-image pairs for pretraining. MSCOCO val set is used for validating pretraining tasks.

Downstream. We consider two datasets for the downstream task, GQA [26] and VQA-HAT [8].

GQA poses visual reasoning in the form of compositional question answering. It requires multihop reasoning to answer the question, so GQA is a special case of VQA. GQA is more diverse than VQA2.0 [15] in terms of coverage of relational, spatial, and multihop reasoning questions. It has 22M QA pairs with 113K images. GQA provides ground truth boxes for question and answer objects making it a suitable test bed for our task.

VQA-HAT dataset provides human attention maps for VQA task. This dataset is based on VQA v1.0 [2] dataset and provides 1374 QA pairs with 488 images in validation set. To evaluate on this dataset, we train our system on VQA v1.0. The answer vocabulary of VQA train set has a long tail distribution. We follow previous works [2, 8] and use 1000 most frequent answers. We first combine training (248,349 QA pairs) and validation data (121,512 QA pairs) to get a total of 368487 QA pairs. We then filter out the questions with out-of-vocabulary answers resulting in 318827 QA pairs.

4.2 Evaluation Metrics

For GQA, VQA accuracy is reported for task accuracy. For grounding task on transformers, we take attention scores from [IMG] token to image from the last cross-attentional layer for all heads. Answer grounding performance is evaluated in terms of the following: **Overlap**– overlap between the ground truth bounding box for answer object and the detected attention region is reported in terms of precision (P), recall (R), and F1-score (F1); **IOU**– intersection over union (IOU) between the ground truth object and detected region is reported in terms of P, R, and F1-score. **Pointing Game**– proposed by [69] is a metric for weakly-supervised visual grounding methods. For pointing game, we consider the point detected from each head as a part of distribution, and perform k-means clustering ($k=1$) on those points. The cluster center is considered as the detected point from the system and used for evaluating accuracy. For VQA-HAT, we report **mean rank correlation** between system generated attention and human attention maps to compare with previous methods.

4.3 Implementation details.

We use $L = 5$ layers in both text and image encoders, and 2 layers in cross-attention module. The transformer encoder layers have the same configuration as BERT with 12 heads and feature dimension $d = 768$. A batch size of 1024 with learning rate $lr = 1e - 4$ is used for pretraining. First stage pretraining is done for 20 epochs and further trained for 10-15 epochs during second stage. We use Imagenet pre-trained ResNet model to extract features of dimensions $7 \times 7 \times 2048$. For finetuning on GQA, we use batch size=32 with $lr = 1e - 5$ and 5-10 training epochs. For VQA-HAT, we use batch size=64 with $lr = 4e - 5$ trained for 20 epochs.

To evaluate the grounding results, we follow the best practice of DINO [4] and take the attention map from the last cross-attentional layer. To compute overlap and IOU for GQA, we threshold over the attention map with an attention threshold of 0.5 to get high attention regions. Each connected region is considered a detection. For pointing game, we find the single cluster center over maximum attention points from all heads and use it for evaluation. We ignore the test samples with empty ground truth maps for pointing game since there is no ground truth bounding box to check for a hit or a miss. For the VQA-HAT evaluation, we follow [8] and use mean rank correlation between the generated attention maps and the ground truth.

4.4 Comparison to State-of-the-Art

We compare the performance of our method to other best-performing methods in the field of weakly supervised VQA grounding and VQA in general, namely MAC [25] and MAC-Caps [28] as representation of visual reasoning architectures, and LXMERT [60], ViLT [31], and ALBEF [36] as state-of-the-art transformer architectures without object features.

Method	Layer	Pointing Game Acc.
Random	-	18.80
Center	-	33.30
MAC [25]	mean	8.90
MAC-Caps [28]	mean	28.46
LXMERT [60]	last	29.00
ALBEF [36]-GC	last	32.13
ALBEF [36]-ATN	last	32.11
ViLT [31]	last	11.99
Ours-no-init (C=16)	last	34.59
Ours-no-init (C=32)	last	34.43
Ours-nogqa (C=32)	last	37.04

Table 1: Pointing game accuracy for GQA. For MAC and MAC-Caps, mean attention maps over reasoning steps are used. For transformer-based methods, maximum attention points from all heads are used for clustering. The cluster center is then used for the pointing game evaluation. For ALBEF, GC=GradCAM output, ATN=attention output. Ours-no-init is the full model with residual connections and trained from scratch, Ours-nogqa uses no GQA samples at pretraining stage. Numbers are reported in percentages.

For LXMERT, we take the provided backbone pre-trained on object features and finetune it using image patches of size $32 \times 32 \times 3$ on GQA. In case of ViLT, we use the provided pre-trained backbone and finetune it on GQA. Following ViLT, we generate a heat map using the cosine similarity between image and word tokens evaluating the similarity scores as well as raw attention for grounding performance for all three metrics. For ALBEF we report results on last layer as well as on layer 8 which is specialized for grounding [36] using the visualizations from gradcam as well as raw attention maps.

GQA We first look at the results of our evaluation on GQA, considering pointing game accuracy in Table 1 and for overlap and IOU in Table 2. Our method outperforms both MAC and MAC-Caps for answer grounding on the last attention map. We achieve an absolute gain of 16.47% (overlap F1-score) and 2.67% increase in IOU F1-score, and an improvement of 25.69% in pointing game accuracy for MAC. When compared with MAC-Caps, our best method (C=16, no-init) improves overlap F1-score by 15.71% \uparrow , IOU F1-score by 2.32% \uparrow , and pointing game accuracy by 6.13% \uparrow . Similar performance gain is observed for question grounding with an improvement of 38.2% \uparrow for overlap F1-score and 3.67% \uparrow gain for IOU F1-score.

To evaluate LXMERT finetuned on image patches (LXMERT-patches), we take the attention score maps from the last cross modality layer. We improve over LXMERT by 12.01% \uparrow absolute points w.r.t overlap F1-score, 2.23% \uparrow w.r.t. IOU F1-score and 5.43% \uparrow gain in pointing game accuracy. For question grounding, LXMERT achieves an overlap F1-score: 43.08% (vs. ours 59.69%) and IOU F1-score of 4.62% (vs. ours 5.96%).

ViLT outperforms all methods in terms of VQA accuracy of 66.33%. However, on the grounding task, it demonstrates the lowest performance for all metrics

Method	Obj.	Backbone	Pre-training	Layer	Acc.	Overlap			IOU		
						P	R	F1	P	R	F1
MAC [25]	A	ResNet	-	last	57.09	5.05	24.44	8.37	0.76	3.70	1.27
MAC-Caps [28]	A	ResNet	-	last	55.13	5.46	27.9	9.13	0.97	4.94	1.62
LXMERT-patches	A	Faster RCNN	MSCO,VG	last	48.65	7.13	64.21	12.83	0.95	8.66	1.71
ALBEF [36]-GC	A	ViT+BERT		last	64.16	6.94	99.92	12.98	0.89	13.43	1.67
ALBEF [36]-ATN	A	ViT+BERT	MSCO,VG,	last	64.20	5.13	99.92	9.75	0.64	12.98	1.21
ALBEF [36]-GC	A	ViT+BERT	SBU,GCC	8	64.20	4.41	99.92	8.44	0.54	12.85	1.04
ALBEF [36]-ATN	A	ViT+BERT		8	64.20	4.82	99.92	9.19	0.60	12.88	1.14
ViLT [32]	A	ViT	MSCO,VG,	last-cos	66.33	0.34	6.13	0.65	0.04	0.63	0.07
ViLT [32]	A	ViT	SBU,GCC	last-ATN	66.33	0.28	4.10	0.53	0.08	1.20	0.15
Ours (C=16)	A	ResNet	MSCO,VG	last	56.65	14.53	85.47	24.84	2.30	13.61	3.94
MAC [25]	Q	ResNet	-	last	57.09	10.79	16.38	13.01	1.39	2.09	1.67
MAC-Caps [28]	Q	ResNet	-	last	55.13	17.39	28.10	21.49	1.87	2.96	2.29
LXMERT-patches	Q	Faster RCNN	MSCO,VG	last	48.65	32.46	64.02	43.08	3.48	6.87	4.62
ALBEF [36]-GC	Q	ViT+BERT		last	64.20	22.15	99.90	36.26	1.96	9.22	3.24
ALBEF [36]-ATN	Q	ViT+BERT	MSCO,VG,	last	64.20	16.50	99.90	28.33	1.40	8.90	2.43
ALBEF [36]-GC	Q	ViT+BERT	SBU,GCC	8	64.20	14.21	99.90	24.88	1.19	8.71	2.09
ALBEF [36]-ATN	Q	ViT+BERT		8	64.20	15.51	99.90	26.85	1.31	8.77	2.27
ViLT [32]	Q	ViT	MSCO,VG,	last-cos	66.33	1.02	5.64	1.73	0.10	0.54	0.17
ViLT [32]	Q	ViT	SBU,GCC	last-ATN	66.33	0.34	1.56	0.56	0.08	0.38	0.14
Ours (C=16)	Q	ResNet	MSCO,VG	last	56.65	47.03	81.67	59.69	4.72	8.08	5.96

Table 2: Results on GQA validation set (for last layer). All methods are evaluated for weak VQA grounding task. For transformer-based models, attention was averaged over all heads. Results are based on grounding of objects referenced in the answer (A) and the question (Q). C=no.of capsules, we report results from our best model with C=16. Refer to table 4 for more variants. For ViLT, we obtain results using cosine similarity (cos.) between text and image features as proposed by the authors as well as from raw attention scores (ATN). For ALBEF, GC is the gradcam output used for evaluation, ATN is the attention output. ALBEF uses layer 8 as grounding layer, we also report grounding performance on this layer. Our method outperforms all baselines for overlap F1-score and IOU F1-score. See section 4.4 for more details. Numbers are reported in percentages.

(table 1: row 7, table 2: rows 8-9). Similar behavior is observed for the question grounding task.

ALBEF produces visualization using GradCAM. We compare with ALBEF using both GradCAM output and attention maps. ALBEF has a very high recall (R) both in terms of overlap and IOU. However, it lacks in precision (P) leading to lower F1-scores for both metrics. Our best model outperforms ALBEF-VQA by a significant margin on both answer grounding and question grounding.

VQA-HAT We further evaluate our system on the VQA-HAT dataset. To this end, we follow the protocol of VQA-HAT and resize the human attention maps and the output attention maps from our system to the common resolution of 14x14. We then rank both of them. VQA-HAT val set provides three human attention maps for each question. We compute the rank correlation of generated attention map with each human attention map and take the average score. Mean rank correlation score over all QA pairs is reported.

Method	Mean Rank-Correlation
Random	0.000 ± 0.001
Human	0.623 ± 0.003
<i>Unsupervised</i>	
SAN [66]	0.249 ± 0.004
HieCoAtt [44]	0.264 ± 0.004
Ours (C=16)	0.479 ± 0.0001
<i>Supervised</i>	
HAN [51]	0.668 ± 0.001

Table 3: Results on VQA-HAT val dataset. *Unsupervised*: no attention supervision, *Supervised*: use attention refinement.

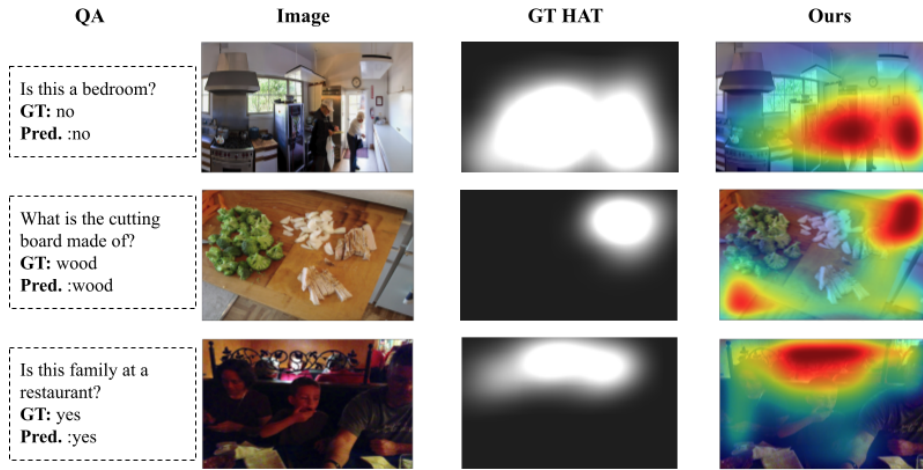


Fig. 3: **Success cases for VQA-HAT dataset.** VQA-HAT provides 3 human attention maps for each image. Here, we show the best matched ground truth map (GT HAT).

We compare our approach on VQA-HAT with three different baselines: SAN [66] and HieCoAtt [44] as unsupervised bounding box free systems, and HAN [51] which uses attention supervision during training. The evaluation is shown in table 3. It shows that the proposed system is able to significantly outperform both methods using VQA-only supervision.

Without any attention supervision during training, we are able to narrow the gap between unsupervised methods and methods such as HAN, which uses human ground truth attention maps during training.

Figure 3 shows success cases on VQA-HAT, comparing our generated attention result to the closest human attention map.

Method	Acc.	Overlap			IOU			Pointing
		P	R	F1	P	R	F1	Game
(1) no skip (C=32)	56.83	11.06	77.60	19.37	1.39	9.85	2.43	29.81
(2) w/skip (C=32)	55.41	10.09	71.95	17.70	1.41	10.09	2.47	34.43
(3) w/skip (C=16)	56.65	14.53	85.47	24.84	2.30	13.61	3.94	34.59
(4) w/skip (C=24)	56.26	10.90	74.03	19.00	1.54	10.56	2.69	31.08
(5) w/skip (C=32)	55.41	10.09	71.95	17.70	1.41	10.09	2.47	34.43
(6) w/skip (C=48)	53.65	10.28	68.94	17.89	1.59	10.73	2.78	29.70
(7) no-init (C=32)	55.41	10.09	71.95	17.70	1.41	10.09	2.47	34.43
(8) vit-bert init (C=32)	58.86	11.11	74.67	19.34	1.55	10.44	2.69	27.06

Table 4: Ablations over the design choices for the proposed architecture on GQA val set. Average attention over all heads in the last transformer layer is used to evaluate the grounding performance. We perform ablation study with C=32 capsules except rows 3-6 where we train the proposed architecture with varying number of capsules. Ablation (1) no skip is our system without residual connections, (2) w/skip is the full model. Rows 7 and 8 is the ablation over weight initialization from pre-trained transformers for vision (ViT) and text (BERT).

4.5 Ablations and Analyses

Impact of Residual Connections. We compare our full system with an ablated variant without residual connections. We observe a drop in performance in terms of overlap, but a slight increase in terms of IOU. Without residual connections, pointing game accuracy is lower than with residual connections (4.62% ↓). We conclude that using residual connections is beneficial for pointing game.

Number of capsules. We ablate our system with varying number of capsules. We train the proposed system with C=16, 24, 32, and 48 capsules. We observe that increase in number of capsules not only decreases VQA accuracy, but also hurts the overlap and IOU in terms of precision, recall and F1-score. Our best method therefore uses 16 capsules with residual connections and pre-trained from scratch.

ViT + BERT + Ours. ViLT and ALBEF initialize their image and text encoders from ViT and/or BERT weights. Although our model is shallow than both models (5 layers in modality specific encoders compared to 12 layers in ViLT and ALBEF), we experimented to initialize our text encoder with BERT weights and image encoder with ViT weights from last 5 layers. We find a gain in VQA accuracy (58.86% vs. 56.65%) but it hurts the grounding performance.

4.6 Qualitative Analysis

In Figure 4, we show some qualitative comparison of our method with the baseline methods. For all examples including the ones where our system predicted the wrong answer, the grounding attention was correct (row 1,4 and 5). Also, the answers are plausible. For instance, in row 3, the correct answer is 'aircraft', and our method predicted it as 'airplane' with the correct localization. Overall, we notice that compared to our method, the baselines were either attending most of

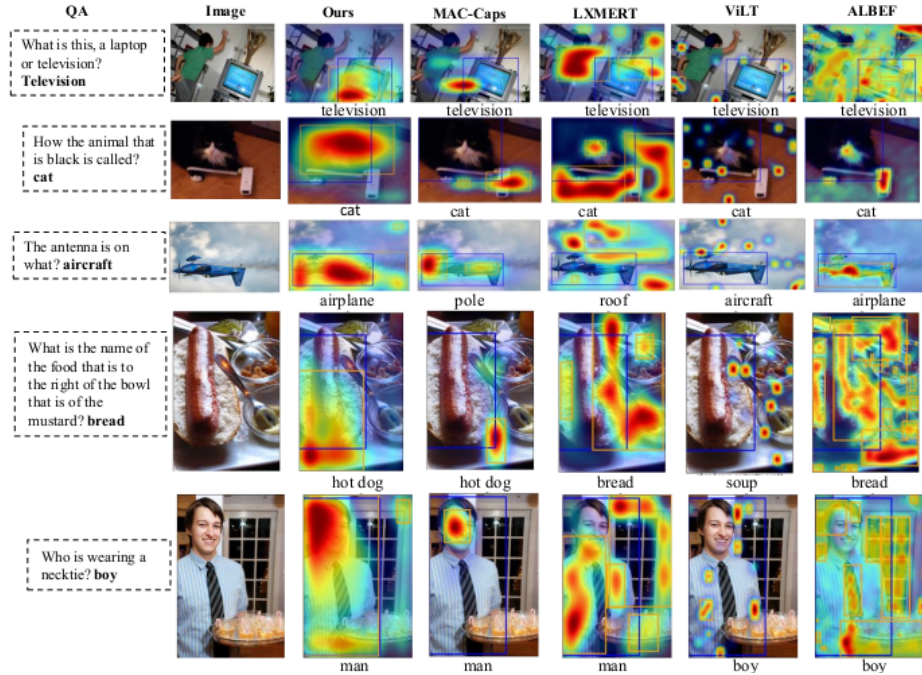


Fig. 4: **Qualitative comparison:** each row shows the input example, and the last layer’s attention visualizations (averaged over all heads) with the predicted answer from all methods. Column 1 shows the question and ground truth answer, column 2 is the input image, column 3 shows the attention output from our method, column 4-7 are results from the baselines. Blue box is the ground truth bounding box for the answer object, orange boxes are the detected regions from each system. We can see that ours is attending relevant answer object with the plausible predicted answer even when the prediction mismatches with the ground truth answer (row 3-5). In row 4, the question is vague; therefore we can say, except LXMERT, all methods choose the correct answer. ALBEF has attention spread over all image which explains the high recall it achieves for overlap and IOU. Refer to section 4.6 for more details and discussion. Best viewed in color.

the image (ALBEF in rows 1,3, and 5 which explains the high recall in table 2), or generate small attention maps (MAC-Caps, ViLT) or looking at the wrong part of the image (LXMERT). More examples and analysis are in the supplementary document.

5 Conclusion

In this work, we show the trade-off between VQA accuracy and the grounding abilities of the existing SOTA transformer-based methods. We propose to use text-guided capsule representation in combination with transformer encoder layers. Our results demonstrate significant improvement over all baselines for all grounding metrics. Extensive experiments demonstrate the effectiveness of the proposed system over the baselines.

References

1. Abacha, A.B., Hasan, S.A., Datla, V.V., Liu, J., Demner-Fushman, D., Müller, H.: Vqa-med: Overview of the medical visual question answering task at imageclef 2019. *CLEF (Working Notes)* **2** (2019)
2. Antol, S., Agrawal, A., Lu, J., Mitchell, M., Batra, D., Zitnick, C.L., Parikh, D.: Vqa: Visual question answering. In: *Proceedings of the IEEE international conference on computer vision*. pp. 2425–2433 (2015)
3. Arbelle, A., Doveh, S., Alfassy, A., Shtok, J., Lev, G., Schwartz, E., Kuehne, H., Levi, H.B., Sattigeri, P., Panda, R., et al.: Detector-free weakly supervised grounding by separation. *arXiv preprint arXiv:2104.09829* (2021)
4. Caron, M., Touvron, H., Misra, I., Jégou, H., Mairal, J., Bojanowski, P., Joulin, A.: Emerging properties in self-supervised vision transformers (2021)
5. Chen, K., Gao, J., Nevatia, R.: Knowledge aided consistency for weakly supervised phrase grounding. In: *Proceedings of the IEEE Conference on Computer Vision and Pattern Recognition*. pp. 4042–4050 (2018)
6. Chen, Y.C., Li, L., Yu, L., El Kholi, A., Ahmed, F., Gan, Z., Cheng, Y., Liu, J.: Uniter: Learning universal image-text representations (2019)
7. Chen, Z., Ma, L., Luo, W., Wong, K.Y.K.: Weakly-supervised spatio-temporally grounding natural sentence in video. *arXiv preprint arXiv:1906.02549* (2019)
8. Das, A., Agrawal, H., Zitnick, C.L., Parikh, D., Batra, D.: Human Attention in Visual Question Answering: Do Humans and Deep Networks Look at the Same Regions? In: *Conference on Empirical Methods in Natural Language Processing (EMNLP)* (2016)
9. Datta, S., Sikka, K., Roy, A., Ahuja, K., Parikh, D., Divakaran, A.: Align2ground: Weakly supervised phrase grounding guided by image-caption alignment. In: *Proceedings of the IEEE/CVF International Conference on Computer Vision*. pp. 2601–2610 (2019)
10. Desai, K., Johnson, J.: VirTex: Learning Visual Representations from Textual Annotations. In: *CVPR* (2021)
11. Devlin, J., Chang, M.W., Lee, K., Toutanova, K.: Bert: Pre-training of deep bidirectional transformers for language understanding. *arXiv preprint arXiv:1810.04805* (2018)
12. Duan, S., Cao, J., Zhao, H.: Capsule-transformer for neural machine translation. *arXiv preprint arXiv:2004.14649* (2020)
13. Duarte, K., Rawat, Y., Shah, M.: Videocapsulenet: A simplified network for action detection. In: *Advances in Neural Information Processing Systems*. pp. 7610–7619 (2018)
14. Duarte, K., Rawat, Y.S., Shah, M.: Capsulevos: Semi-supervised video object segmentation using capsule routing. In: *Proceedings of the IEEE International Conference on Computer Vision*. pp. 8480–8489 (2019)
15. Goyal, Y., Khot, T., Summers-Stay, D., Batra, D., Parikh, D.: Making the v in vqa matter: Elevating the role of image understanding in visual question answering. In: *Proceedings of the IEEE Conference on Computer Vision and Pattern Recognition*. pp. 6904–6913 (2017)
16. Gu, S., Feng, Y.: Improving multi-head attention with capsule networks. In: *CCF International Conference on Natural Language Processing and Chinese Computing*. pp. 314–326. Springer (2019)
17. Gurari, D., Li, Q., Stangl, A.J., Guo, A., Lin, C., Grauman, K., Luo, J., Bigham, J.P.: Vizwiz grand challenge: Answering visual questions from blind people. In:

- Proceedings of the IEEE Conference on Computer Vision and Pattern Recognition. pp. 3608–3617 (2018)
18. Hinton, G.: Some demonstrations of the effects of structural descriptions in mental imagery. *Cognitive Science* **3**(3), 231–250 (1979)
 19. Hinton, G.: How to represent part-whole hierarchies in a neural network. arXiv preprint arXiv:2102.12627 (2021)
 20. Hinton, G.E., Krizhevsky, A., Wang, S.D.: Transforming auto-encoders. In: International conference on artificial neural networks. pp. 44–51. Springer (2011)
 21. Hinton, G.E., Sabour, S., Frosst, N.: Matrix capsules with em routing. In: International conference on learning representations (2018)
 22. Huang, D.A., Buch, S., Dery, L., Garg, A., Fei-Fei, L., Niebles, J.C.: Finding" it": Weakly-supervised reference-aware visual grounding in instructional videos. In: Proceedings of the IEEE Conference on Computer Vision and Pattern Recognition. pp. 5948–5957 (2018)
 23. Huang, Z., Zeng, Z., Huang, Y., Liu, B., Fu, D., Fu, J.: Seeing out of the box: End-to-end pre-training for vision-language representation learning. In: The IEEE Conference on Computer Vision and Pattern Recognition (CVPR) (2021)
 24. Huang, Z., Zeng, Z., Liu, B., Fu, D., Fu, J.: Pixel-bert: Aligning image pixels with text by deep multi-modal transformers. CoRR **abs/2004.00849** (2020), <https://arxiv.org/abs/2004.00849>
 25. Hudson, D.A., Manning, C.D.: Compositional attention networks for machine reasoning. International Conference on Learning Representations (ICLR) (2018)
 26. Hudson, D.A., Manning, C.D.: Gqa: A new dataset for real-world visual reasoning and compositional question answering. Conference on Computer Vision and Pattern Recognition (CVPR) (2019)
 27. Kahneman, D., Treisman, A., Gibbs, B.J.: The reviewing of object files: Object-specific integration of information. *Cognitive psychology* **24**(2), 175–219 (1992)
 28. Khan, A.U., Kuehne, H., Duarte, K., Gan, C., Lobo, N., Shah, M.: Found a reason for me? weakly-supervised grounded visual question answering using capsules (2021)
 29. Khan, S., Naseer, M., Hayat, M., Zamir, S.W., Khan, F.S., Shah, M.: Transformers in vision: A survey. arXiv preprint arXiv:2101.01169 (2021)
 30. Khan, S., Naseer, M., Hayat, M., Zamir, S.W., Khan, F.S., Shah, M.: Transformers in vision: A survey. arXiv preprint arXiv:2101.01169 (2021)
 31. Kim, W., Son, B., Kim, I.: Vilt: Vision-and-language transformer without convolution or region supervision. In: Meila, M., Zhang, T. (eds.) Proceedings of the 38th International Conference on Machine Learning. Proceedings of Machine Learning Research, vol. 139, pp. 5583–5594. PMLR (18–24 Jul 2021), <http://proceedings.mlr.press/v139/kim21k.html>
 32. Kim, W., Son, B., Kim, I.: Vilt: Vision-and-language transformer without convolution or region supervision. In: Meila, M., Zhang, T. (eds.) Proceedings of the 38th International Conference on Machine Learning. Proceedings of Machine Learning Research, vol. 139, pp. 5583–5594. PMLR (18–24 Jul 2021), <http://proceedings.mlr.press/v139/kim21k.html>
 33. Krishna, R., Zhu, Y., Groth, O., Johnson, J., Hata, K., Kravitz, J., Chen, S., Kalantidis, Y., Li, L.J., Shamma, D.A., et al.: Visual genome: Connecting language and vision using crowdsourced dense image annotations. *International journal of computer vision* **123**(1), 32–73 (2017)
 34. LaLonde, R., Bagci, U.: Capsules for object segmentation. arXiv preprint arXiv:1804.04241 (2018)

35. Li, G., Duan, N., Fang, Y., Gong, M., Jiang, D.: Unicoder-vl: A universal encoder for vision and language by cross-modal pre-training. In: *Proceedings of the AAAI Conference on Artificial Intelligence*. vol. 34, pp. 11336–11344 (2020)
36. Li, J., Selvaraju, R.R., Gotmare, A.D., Joty, S., Xiong, C., Hoi, S.: Align before fuse: Vision and language representation learning with momentum distillation. In: *NeurIPS* (2021)
37. Li, L.H., Yatskar, M., Yin, D., Hsieh, C.J., Chang, K.W.: Visualbert: A simple and performant baseline for vision and language. *arXiv preprint arXiv:1908.03557* (2019)
38. Li, X., Yin, X., Li, C., Zhang, P., Hu, X., Zhang, L., Wang, L., Hu, H., Dong, L., Wei, F., et al.: Oscar: Object-semantics aligned pre-training for vision-language tasks. In: *European Conference on Computer Vision*. pp. 121–137. Springer (2020)
39. Lin, T.Y., Maire, M., Belongie, S., Hays, J., Perona, P., Ramanan, D., Dollár, P., Zitnick, C.L.: Microsoft coco: Common objects in context. In: *European conference on computer vision*. pp. 740–755. Springer (2014)
40. Liu, J., Lin, H., Liu, X., Xu, B., Ren, Y., Diao, Y., Yang, L.: Transformer-based capsule network for stock movement prediction. In: *Proceedings of the First Workshop on Financial Technology and Natural Language Processing*. pp. 66–73 (2019)
41. Liu, Y., Wan, B., Ma, L., He, X.: Relation-aware instance refinement for weakly supervised visual grounding. In: *Proceedings of the IEEE/CVF Conference on Computer Vision and Pattern Recognition*. pp. 5612–5621 (2021)
42. Lu, J., Batra, D., Parikh, D., Lee, S.: Vilbert: Pretraining task-agnostic visiolinguistic representations for vision-and-language tasks. *arXiv preprint arXiv:1908.02265* (2019)
43. Lu, J., Goswami, V., Rohrbach, M., Parikh, D., Lee, S.: 12-in-1: Multi-task vision and language representation learning. In: *Proceedings of the IEEE/CVF Conference on Computer Vision and Pattern Recognition*. pp. 10437–10446 (2020)
44. Lu, J., Yang, J., Batra, D., Parikh, D.: Hierarchical question-image co-attention for visual question answering. *Advances in neural information processing systems* **29** (2016)
45. Mazzia, V., Salvetti, F., Chiaberge, M.: Efficient-capsnet: Capsule network with self-attention routing. *arXiv preprint arXiv:2101.12491* (2021)
46. Miech, A., Alayrac, J.B., Laptev, I., Sivic, J., Zisserman, A.: Thinking fast and slow: Efficient text-to-visual retrieval with transformers. In: *Proceedings of the IEEE/CVF Conference on Computer Vision and Pattern Recognition*. pp. 9826–9836 (2021)
47. Mobiny, A., Cicalese, P.A., Nguyen, H.V.: Trans-caps: Transformer capsule networks with self-attention routing (2021), <https://openreview.net/forum?id=BUPIRa1D2J>
48. Niu, Y., Tang, K., Zhang, H., Lu, Z., Hua, X.S., Wen, J.R.: Counterfactual vqa: A cause-effect look at language bias. In: *Proceedings of the IEEE/CVF Conference on Computer Vision and Pattern Recognition*. pp. 12700–12710 (2021)
49. Pfeiffer, J., Geigle, G., Kamath, A., Steitz, J.M.O., Roth, S., Vulić, I., Gurevych, I.: xgqa: Cross-lingual visual question answering. *arXiv preprint arXiv:2109.06082* (2021)
50. Pucci, R., Micheloni, C., Martinel, N.: Self-attention agreement among capsules. In: *Proceedings of the IEEE/CVF International Conference on Computer Vision*. pp. 272–280 (2021)
51. Qiao, T., Dong, J., Xu, D.: Exploring human-like attention supervision in visual question answering. In: *Proceedings of the AAAI Conference on Artificial Intelligence*. vol. 32 (2018)

52. Radford, A., Kim, J.W., Hallacy, C., Ramesh, A., Goh, G., Agarwal, S., Sastry, G., Askell, A., Mishkin, P., Clark, J., Krueger, G., Sutskever, I.: Learning transferable visual models from natural language supervision (2021)
53. Ramakrishnan, S., Agrawal, A., Lee, S.: Overcoming language priors in visual question answering with adversarial regularization. arXiv preprint arXiv:1810.03649 (2018)
54. Ribeiro, F.D.S., Duarte, K., Everett, M., Leontidis, G., Shah, M.: Learning with capsules: A survey. arXiv preprint arXiv:2206.02664 (2022)
55. Riquelme, F., De Goyeneche, A., Zhang, Y., Niebles, J.C., Soto, A.: Explaining vqa predictions using visual grounding and a knowledge base. *Image and Vision Computing* **101**, 103968 (2020)
56. Sabour, S., Frosst, N., Hinton, G.E.: Dynamic routing between capsules. In: *NIPS* (2017)
57. Selvaraju, R.R., Lee, S., Shen, Y., Jin, H., Ghosh, S., Heck, L., Batra, D., Parikh, D.: Taking a hint: Leveraging explanations to make vision and language models more grounded. In: *Proceedings of the IEEE/CVF International Conference on Computer Vision*. pp. 2591–2600 (2019)
58. Shi, J., Xu, J., Gong, B., Xu, C.: Not all frames are equal: Weakly-supervised video grounding with contextual similarity and visual clustering losses. In: *Proceedings of the IEEE/CVF Conference on Computer Vision and Pattern Recognition*. pp. 10444–10452 (2019)
59. Su, W., Zhu, X., Cao, Y., Li, B., Lu, L., Wei, F., Dai, J.: Vl-bert: Pre-training of generic visual-linguistic representations. arXiv preprint arXiv:1908.08530 (2019)
60. Tan, H., Bansal, M.: Lxmert: Learning cross-modality encoder representations from transformers. In: *Proceedings of the 2019 Conference on Empirical Methods in Natural Language Processing* (2019)
61. Wang, L., Huang, J., Li, Y., Xu, K., Yang, Z., Yu, D.: Improving weakly supervised visual grounding by contrastive knowledge distillation. In: *Proceedings of the IEEE/CVF Conference on Computer Vision and Pattern Recognition*. pp. 14090–14100 (2021)
62. Whitehead, S., Wu, H., Ji, H., Feris, R., Saenko, K.: Separating skills and concepts for novel visual question answering. In: *Proceedings of the IEEE/CVF Conference on Computer Vision and Pattern Recognition (CVPR)*. pp. 5632–5641 (June 2021)
63. Wu, L., Liu, X., Liu, Q.: Centroid transformers: Learning to abstract with attention. arXiv preprint arXiv:2102.08606 (2021)
64. Xiao, F., Sigal, L., Jae Lee, Y.: Weakly-supervised visual grounding of phrases with linguistic structures. In: *Proceedings of the IEEE Conference on Computer Vision and Pattern Recognition*. pp. 5945–5954 (2017)
65. Yang, X., Liu, X., Jian, M., Gao, X., Wang, M.: Weakly-supervised video object grounding by exploring spatio-temporal contexts. In: *Proceedings of the 28th ACM International Conference on Multimedia*. pp. 1939–1947 (2020)
66. Yang, Z., He, X., Gao, J., Deng, L., Smola, A.: Stacked attention networks for image question answering. In: *Proceedings of the IEEE conference on computer vision and pattern recognition*. pp. 21–29 (2016)
67. Zeng, X., Wang, Y., Chiu, T.Y., Bhattacharya, N., Gurari, D.: Vision skills needed to answer visual questions. *Proceedings of the ACM on Human-Computer Interaction* **4**(CSCW2), 1–31 (2020)
68. Zhan, L.M., Liu, B., Fan, L., Chen, J., Wu, X.M.: Medical visual question answering via conditional reasoning. In: *Proceedings of the 28th ACM International Conference on Multimedia*. pp. 2345–2354 (2020)

69. Zhang, J., Bargal, S.A., Lin, Z., Brandt, J., Shen, X., Sclaroff, S.: Top-down neural attention by excitation backprop. *International Journal of Computer Vision* **126**(10), 1084–1102 (2018)
70. Zhang, S., Qu, L., You, S., Yang, Z., Zhang, J.: Automatic generation of grounded visual questions. *arXiv preprint arXiv:1612.06530* (2016)
71. Zhang, Y., Niebles, J.C., Soto, A.: Interpretable visual question answering by visual grounding from attention supervision mining. In: 2019 IEEE Winter Conference on Applications of Computer Vision (WACV). pp. 349–357 (2019). <https://doi.org/10.1109/WACV.2019.00043>
72. Zhu, Y., Groth, O., Bernstein, M., Fei-Fei, L.: Visual7w: Grounded question answering in images. In: *Proceedings of the IEEE conference on computer vision and pattern recognition*. pp. 4995–5004 (2016)

Supplementary: Weakly Supervised Grounding for VQA in Vision-Language Transformers

In this supplementary document, we further discuss about the proposed work as follows:

- Additional implementation details (section A)
- Additional architecture details (section B)
- Training objectives’ details (section C)
- Grounding Performance Evaluation (section D)
- Performance analysis w.r.t. varying detection threshold (section E)
- Grounding accuracy w.r.t. each head (section F)
- Results w.r.t. question type (section G)
- Entities represented by visual capsules (section H)
- Training parameters in our method (section I)
- VQA accuracy comparison (section J)
- Additional details about evaluation on VQA-HAT (section K)
- Qualitative Results (section L)

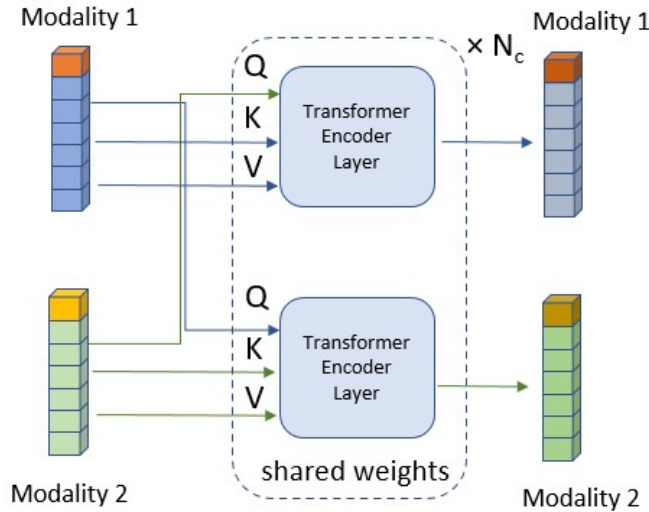


Fig. 5: Cross-attentional module used in our architecture. We use two cross-attentional layers, i.e., $N_c = 2$ in our best model.

A Additional Implementation details

Here, we discuss the additional design choices used in our model. The capsules use routing to agree or disagree about the presence of certain entities in the input

image. This decision is independent of the question. For instance, if an image has a *bus* and an *elephant* in it, the question cannot affect what is in the image. To this end, the capsule routing is performed only once in our method. However, depending on the question being asked, we may require selecting different entities from the image. We achieve this by doing text-based capsule selection at each layer. The capsule selection layer ϕ (equation 3 in the main paper) has shared weights for all encoder layers. We use 8 16GB AMD GPUs for pretraining; finetuning for GQA is performed on a single 16GB GPU. To pretrain with 48 capsules, the batch size of 640 is used.

B Additional Architectural details

Language Encoder: The language encoder L_e is composed of L transformer encoder layers. Its input is a tokenized sentence S_l of length l . The language encoder L_e takes the set of words tokens $\{[CLS], w_1, w_2, \dots, w_l, [SEP]\}$ as input, and outputs feature representations $\{h_{cls}^i, h_{T_1}^i, h_{T_2}^i, \dots, h_{T_l}^i, h_{sep}^i\}$ at every i^{th} layer, where $h_{T_k}^i$ denotes the text feature for the k^{th} input word token ($k \in 1, 2, \dots, l$) from layer i . Intermediate encoder layer i takes output of previous layer ($i - 1$) as input. $[CLS]$ token is used as the sentence embedding in transformers [11]. Additionally, we use it for capsule selection in visual encoder (section 3.3 in main).

Visual Encoder: The visual encoder V_e has the same architecture as the language encoder with the same dimension size and number of layers. The image embeddings X' are transformed to visual capsules encodings X_c and input to the visual encoder. Intermediate layers of visual encoder takes selected visual capsules as residual connection to keep the capsule representation intact while training the system. The final features output $h_{v_j}^L$ of the visual encoder is used for token-level cross-modality interactions in future steps. Where, $h_{v_j}^L$ is the feature output for j^{th} visual token ($j \in 1, 2, \dots, hw$) from the last layer L .

Feature Pooling The feature pooling layer takes text-based features and image-based features as input and outputs a d dimensional feature. This output feature can be used as a pooled output for image-text matching and VQA tasks. The feature pooling layer is a fully connected layer followed by a \tanh activation layer. We pretrain our system in two stages before finetuning for VQA task. To be specific, during first stage pretraining, the input is the concatenated features $[h_{cls}^L, h_{img}^L]$ for special tokens from text and image encoders; where h_{cls}^L , and h_{img}^L are used as aggregated features over text input and image input respectively. Let f_P be the feature pooling layer, the pooled feature output $h_{1_{pooled}}$ will be as follows:

$$h_{1_{pooled}} = f_P([h_{cls}^L, h_{img}^L]) \quad (7)$$

During second stage pretraining, the concatenated features pair after cross attention is indicated as $[h_{cls}^{\hat{L}}, h_{img}^{\hat{L}}]$ and the pooled feature output is denoted by $h_{2_{pooled}}$. The equation is as follows:

$$h_{2_{pooled}} = f_P(h_{cls}^{\hat{L}}, h_{img}^{\hat{L}}) \quad (8)$$

Cross-Attention Module Given two input feature sequences (output $h_{T_k}^L$ from text encoder and $h_{v_j}^L$ from image encoder), cross-attention module is a co-attentional transformer which applies attention from one feature sequence to the other by taking queries from first sequence and keys and values from the second sequence, and vice versa. Multiple layers of these cross-attention blocks can be stacked. The final text output feature $h_{cls}^{\hat{L}}$ corresponding to the $[CLS]$ token and final visual output feature $h_{img}^{\hat{L}}$ corresponding to the $[IMG]$ token are used for pretraining and finetuning the model. Where, N_c is the number of layers in cross-attention module and $\hat{L} = L + N_c$ denotes the depth of the model in terms of number of layers.

C Training objectives

Masked Language Modeling Masked Language Modeling is a self-supervised language modeling task where a small percentage of words are masked before giving the sentence as input to the language encoder. The task is to predict the masked words using the context from other words in the sentence. This self-supervised approach is very effective to learn strong text representations [11]. The features output $h_{T_k}^L$ from language encoder L_e is used for training on this task. In the second stage, instead of predicting missing words from solely text features, the masked word is predicted from the visual-guided language features i.e., we take features outputs $h_k^{\hat{L}}$ from the last text-based cross-attention layer.

Image-Text Matching (ITM) To predict whether the input pair of image-text features is a matching pair or not, we take the output $h_{1_{pooled}}$ (eq. 7) from feature pooling layer and input to a fully connected layer which outputs logits for each class: 'matching' or 'non-matching'. At the second pretraining stage, the output features corresponding to $[IMG]$ and $[CLS]$ token after cross-attentional module (each of dimension d) are used for prediction. The pretraining head now uses $h_{2_{pooled}}$ (eq. 8) as input for image-text matching task.

Visual Question Answering Inspired by [60], we also use VQA as one of our pretraining tasks. We use Visual7W [72], GQA [26] and VQA [15] in our pretraining. Like ITM, we take the pooled features from text and visual encoders and input to a classifier. The classifier is comprised of two fully connected layers. An activation function and layer norm is used between the two layers. The final output is probability scores for each answer. In the first stage of pretraining, $h_{1_{pooled}}$ is used as the pooled feature. For second stage pretraining, pooled cross-modal feature output $h_{2_{pooled}}$ is used for answer prediction. A separate softmax cross-entropy loss function is used to optimize each of the above heads. We give equal weights to each loss term during pretraining.

Finetuning parameters for the baselines. To finetune LXMERT, we use the same training parameters as our method. ViLT is finetuned with batch size of 256 with $lr=1e-5$. ALBEF is finetuned with batch size of 16. Learning rate is increased to $2e-5$ to speed up training for ALBEF. ALBEF and ViLT use the maximum batch size which could fit in the GPU memory. All models are trained on GQA for upto 10 epochs.

Obj. label	Overlap			IOU		
	P	R	F1	P	R	F1
Answer (A)	17.64	89.81	29.49	2.05	10.45	3.42
Question (Q)	49.57	81.86	61.75	4.01	6.48	4.95

Table 5: GradCAM results for our model. Compare to Tab. 2 in the paper.

D Grounding Performance Evaluation

Choice to use last layer’s attention for grounding: It is common in the vision-language community to employ the last layer’s analysis e.g., DINO [4] uses the last layer’s attention for the object segmentation task without any specialized training objective or architecture. We follow the protocol of previous works in the field for SOTA comparison to allow for a fair evaluation, namely following MAC [25], MAC-Caps [28] with mean (last) attention scores, ALBEF [36] by using the 8th and last layer with Grad-CAM (GC) and attention scores (ATN) and ViLT [31] for the last layer cosine (cos) and attention scores (see Tab. 2 in the main paper) and achieve SOTA grounding performance. However, there is a possibility that some intermediate layer does the better job at grounding such as ALBEF finds that layer 8 in their model is good at grounding. Nevertheless, searching for the best layer is expensive in terms of time and computational cost. Our approach outperforms on grounding even when evaluated for the last layer only. This choice also eliminates the need to search for the best grounding layer within each model and well suited to test the systems for unseen data.

Ours + Grad-CAM: To compare with ALBEF, we also evaluated our system with Grad-CAM output of the last layer. We observe $\approx 2 - 4\%$ \uparrow increase in overlap F1-score for both Q & A and a ($\approx 0.5 - 1.01\%$ \downarrow) decrease in IOU F1-score still achieving better grounding results than the baselines (see Tab. 5 and Tab. 2 (main)).

Generating heatmaps using ViLT demo: The demo code visualizes word-to-patch attention for the matching image-caption pair. For VQA grounding, we consider question-to-image attention (attention from [CLS] token to visual tokens). The provided code for optimal transport algorithm leads to numerical instability for the question token ([CLS]) generating NaN. Hence, we used the cosine scores (computed before optimal transport) as well as raw attention to generate heatmaps. Heatmaps are generated with the same post processing as provided in the demo. To verify this, ($< question_id >$, $< image_id >$) pairs for Fig.4 (main) are: $\{('00798998', '2356417'), ('02451905', '2386586'), ('00653991', '2324955'), ('00511505', '2410567'), ('01782610', '2409395')\}$.

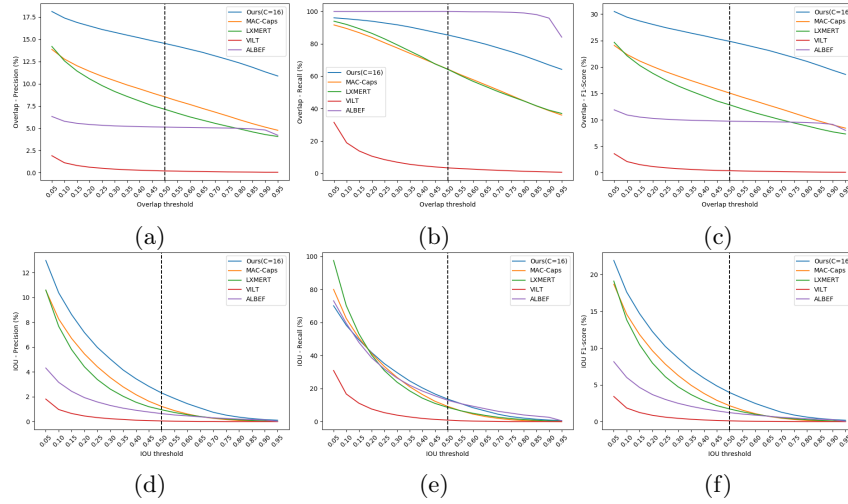


Fig. 6: Comparison with baselines for varying overlap and IOU detection threshold from 0.05 to 0.95. Plots (a), (b), and (c) show the results for varying detection threshold for overlap in terms of precision, recall, and F1-score respectively. Plots (d), (e), and (f) are the results for comparison when varying IOU threshold in terms of precision, recall, and F1-score respectively. Our method is significantly outperforming the baselines for all values of overlap thresholds in terms of precision, and subsequently F1-scores. For IOU, the proposed method is doing well for threshold values as high as 0.8 in terms of precision and F1-score, whereas, IOU-Recall is comparable to ALBEF.

E Performance analysis w.r.t. varying detection threshold

We use detection threshold=0.5 for all our results in the submitted paper. For overlap, a detection is considered to be a true positive when the overlap between the ground truth box and the predicted region is greater than 0.5. Similarly, a detected region with an IOU of greater than 0.5 over a ground truth bounding box is considered a true positive for IOU. In figure 6, we study the impact of having a very low detection threshold vs. employing high thresholds by varying the threshold from 0.05 upto 0.95. We observe that the proposed method is robust to detection threshold for the overlap metric in terms of precision and F1-score even for the very high threshold of 0.95. For IOU, we also perform well for precision and F1-score. For IOU in terms of recall, our method and ALBEF show comparable results.

F Grounding accuracy w.r.t. each head

Grounding accuracy for individual heads in the last cross-attentional layer are shown in figure 7. The results are reported in terms of precision, recall, and F1-score for overlap and IOU. For pointing game, the maximum point over the attention map produced from each head is used to evaluate the per-head

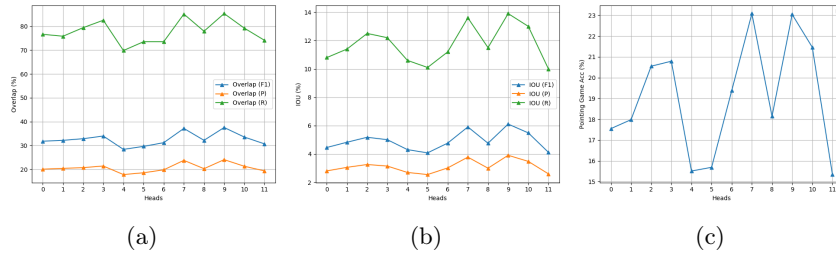


Fig. 7: Grounding performance from the proposed model ($C=16$) for each head in the last cross-attention layer. (a) reports overlap accuracies in terms of precision, recall, and F1-score; (b) shows IOU in terms of precision, recall, and F1-score; and (c) shows pointing game accuracy for each head. Overall, head 7 and head 10 show best grounding performance among all heads. For pointing game, head 7 achieves the highest accuracy of 23.08%. Using the proposed way to evaluate the pointing game performance, i.e., clustering over maximum points from all heads, improves pointing game accuracy significantly (34.59%).

pointing game accuracy. Using clustering over the points obtained from each head outperforms the best performing head by $\uparrow 11.51\%$ (best head: 23.08% vs. clustering: 34.59%).

G Results w.r.t. question type

Table 6 shows grounding results of our best model for different question types. GQA has questions classified with respect to structural type and semantic type. We compare our model with our backbone model which uses no capsules. Our system outperforms over all question types for both overlap and IOU particularly for question type “compare”, “choose”, and “attribute”. Examples for each question type are provided in table 6. Refer to GQA [26] for more details about the question types present in this dataset.

H Entities represented by capsules

Since, we do not use class labels to train the capsules, and use VQA supervision instead for training the whole system, it is hard to guess which entity is being represented by each capsule. To examine what individual capsules are learning, we take the average over capsule activations for each spatial location resulting in a vector of dimension C (C =number of capsules). Each feature in that C -dimensional vector shows the average activation (presence probability) of an individual capsule for that image. The highest activated capsule is used to sort the images into C groups. Figure 8 shows the images where a given capsule had the highest activation. In the figure, we can see different capsules are focused on different types of images, e.g., capsule 1 is mostly focused on *outdoor sports* like *surfing*. Since these capsule representations are learned in a weakly-supervised

Q Type	Example	Method	Acc.	Overlap			IOU		
				P	R	F1	P	R	F1
Open	<i>How is the weather in the image?</i>	no-caps	62.43	23.03	46.02	30.70	4.83	9.66	6.44
		ours	56.65	43.06	85.57	57.29	6.62	13.24	8.83
Binary	<i>Is it cloudy today?</i>	no-caps	62.43	33.19	66.10	44.20	7.13	14.25	9.50
		ours	56.65	42.54	84.67	56.63	12.12	24.23	16.15
Query	<i>What kind of fruit is on the table?</i>	no-caps	62.43	33.19	66.10	44.20	4.83	9.66	6.44
		ours	56.65	43.06	85.57	57.29	6.62	13.24	8.83
Compare	<i>Who is taller, the boy or the girl?</i>	no-caps	62.43	9.96	19.91	13.27	1.11	2.21	1.47
		ours	56.65	37.83	75.00	50.29	2.43	4.87	3.24
Choose	<i>Is it sunny or cloudy?</i>	no-caps	62.43	24.62	49.19	32.82	7.86	15.72	10.48
		ours	56.65	43.11	85.85	57.40	13.29	26.59	17.73
Category	<i>What kind of fruit is it, an apple or a banana?</i>	no-caps	62.43	30.14	60.10	40.14	8.66	17.32	11.54
		ours	56.65	42.90	85.49	57.13	11.73	23.46	15.64
Relation	<i>Is there an apple on the black table?</i>	no-caps	62.43	33.45	66.60	44.53	4.16	8.31	5.54
		ours	56.65	43.10	85.60	57.33	5.84	11.68	7.79
Attribute	<i>what color is the apple?</i>	no-caps	62.43	9.96	19.91	13.27	1.11	2.21	1.47
		ours	56.65	37.83	75.00	50.29	2.43	4.87	3.24

Table 6: Comparison of our backbone model with no capsules (no-caps) and the proposed model with 16 capsules (Ours (C=16)). Results are shown w.r.t. each question type. Adding capsules to the backbone model significantly improves the grounding performance for all question types.

Method	depth (#transformer layers)	#Params (M)
LXMERT [60]	12	239.8
ALBEF [36]	12	209.5
ViLT [31]	12	87.4
Ours	7	141.0

Table 7: Number of parameters in all transformer-based methods.

manner, they show overlapping behavior over certain image classes. Some of them exhibit an interesting behavior. For instance, while capsule 2 is focused on *food items*, capsule 9 is fond of *pizza*; capsule 5 has learned what an *elephant* looks like, but also good at identifying *giraffes* and *cows* in the wild; capsule 13 is focused on *buildings*. We used our best model with C=16 capsules for these visualizations.

I No. of training parameters

We compare the proposed model with other transformer-based methods in table 7. Our proposed system is shallower than the baseline methods using 5 layers in each modality-specific encoders followed by 2 cross-attentional layers. We denote the length of a vertical stack of transformer layers as the model’s *depth*. We follow [31, 60] and consider one single modality layer as 1/2 of a multimodal layer.

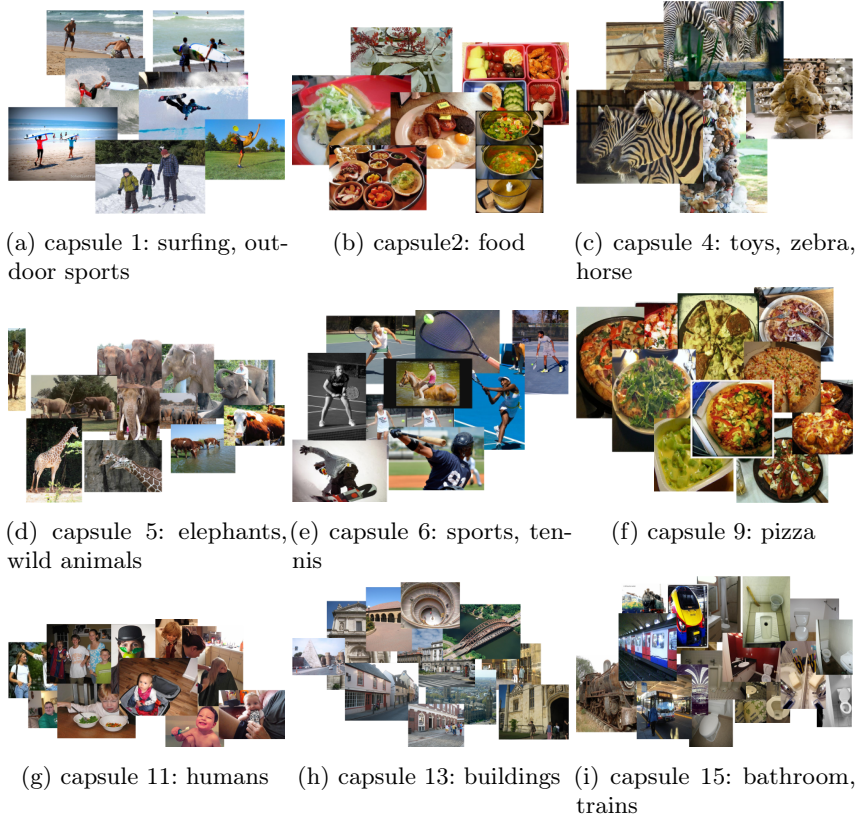


Fig. 8: Images represented by individual capsules. Here, we show the group of images where a certain capsule has the highest activation, e.g., capsule 9 has the highest activation when there is *pizza* in the image.

Hence, the proposed model has the depth=7 compared to the baselines with depth=12. In comparison to other transformer-methods, the proposed system uses less parameters ($\approx 141\text{M}$) than LXMERT [60] (239.8M) and ALBEF [36] (209.5M). ViLT has the least number of parameters (87.4M). However, it is a single stream model compared to all other two-stream methods considered for this work including the proposed architecture. We excluded the text embedding layer when computing the number of training parameters since it is shared among all vision-language transformers which are used in this study [31].

J VQA accuracy of ours vs. baselines:

Our proposed system while achieving better VQA accuracy than previous grounding SOTA on GQA dataset (MAC-Caps [28]) and LXMERT (a transformer-based model with object-detection), performs lower than ViLT and ALBEF. We attribute this to two reasons: 1) Less training data – ViLT and ALBEF are using

<i>Answer Plausibility</i>	ALBEF	ViLT	Ours
<i>for all</i>	92.12	92.28	92.30
<i>for mispredicted</i>	85.14	86.35	87.15

Table 8: Plausibility comparison on GQA-val set with ALBEF and ViLT for all question-answer pairs and the mispredicted question-answer pairs. We perform on par (even slightly better) than the baselines in terms of the predicted answer’s plausibility. This verifies the system is predicting reasonable answers in the real-world context.

SBU and GCC additionally with strong data augmentations, so we assume that using additional data and comparable resources for training would improve our accuracy as well. 2) Considering failure cases in more detail, we find that the lower accuracy is mainly driven by semantically correct, but literally wrong answers such as girl vs women or herd vs cow (see examples in Fig. 9, 12, and 11). The answer prediction despite being reasonable is incorrect in terms of language mismatch with the ground truth. It could be possible that capsules help to prevent dataset biases, as they regularize and constrain the training and therefore suppress "shortcuts" based on dataset noise. To validate this further, we compute the plausibility metric for all questions as well as incorrect predictions. **Plausibility** measures that an answer is reasonable in the real-world context e.g., it is unlikely to see a ‘blue’ apple in real-world. We perform on par with ViLT and ALBEF for all predicted answers. When compared on the mispredicted questions for all three methods, our system predicts 2% more plausible answers than ALBEF and 0.8% better than ViLT (see table 8). This study maintains the observation about the predicted answer while being reasonable in the real-world is considered incorrect in terms of exact match with the ground truth consequently leading to decreased VQA accuracy.

K Additional details about evaluation on VQA-HAT dataset

VQA-HAT dataset provides human attention maps for VQA task. This dataset is based on VQA v1.0 dataset and provides 1473 QA pairs with 488 images in validation set. To evaluate on this dataset, we train our system on VQA v1.0 and evaluate on VQA-HAT validation set. The answer vocabulary of VQA train set has a long tail distribution. We follow previous works [2, 8] and use 1000 most frequent answers. We first combine training (248,349 QA pairs) and validation data (121,512 QA pairs) to get a total of 368487 QA pairs. We then filter out the questions with out-of-vocabulary answers (answer vocab size is kept 1K) resulting in 318827 QA pairs. We separate out 10K QA pairs from the training set (after above mentioned question filtering) and use it as a validation set to pick our best model. We therefore use 308K QA pairs from VQA v1.0 train and val set for finetuning our pretrained backbone with 16 capsules. The learning parameters

used for this training are $\text{lr}=4\text{e-}5$, $\text{batch size}=64$, with bert optimizer and trained for 20 epochs. The best model on validation set is used for evaluation.

L Qualitative Results

In figure 9 and 10, we show more examples for qualitative comparison with baselines. Our system consistently produces correct grounding attention when compared to the baselines. In figure 11, we show some failure cases for our system in terms of grounding output as well as answer prediction. For grounding failure (in terms of IOU with the groundtruth box), we observe that the system’s attention is cogent. For instance, in the top left example, for the question *where is the giraffe?*, the system is looking at the surroundings of giraffe and predicting the answer *zoo*. In the right two examples, the system is grounding correctly even generating reasonable answers. However, these answers are considered incorrect in terms of language mismatch with the groundtruth answer (herd vs. cow and beach vs. sand). Finally, in figure 12, we present more qualitative examples from our system.

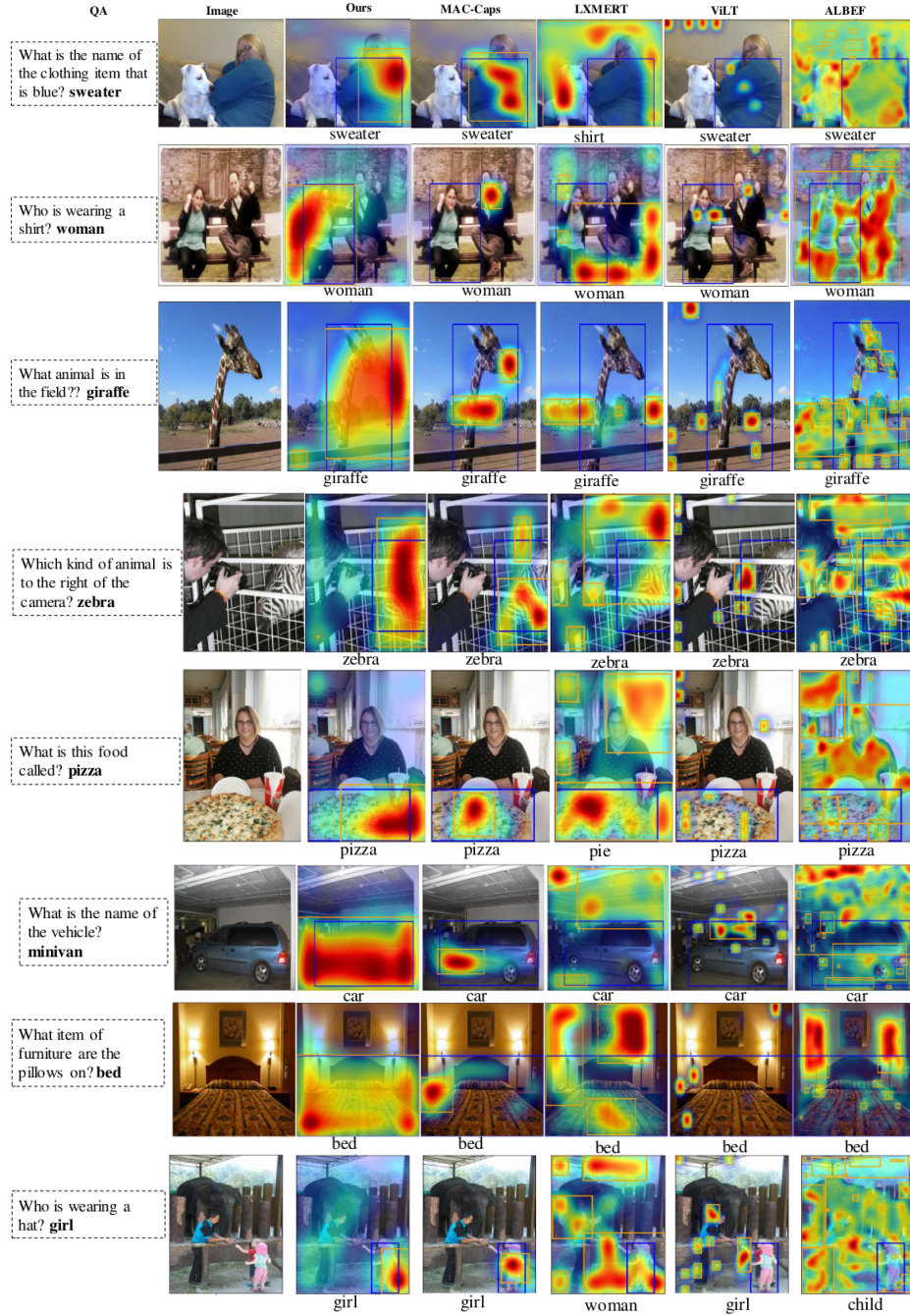


Fig. 9: More qualitative examples where the model predicted the answer correctly with attention (with detected orange boxes) on the correct image regions (blue boxes). Best viewed in color.

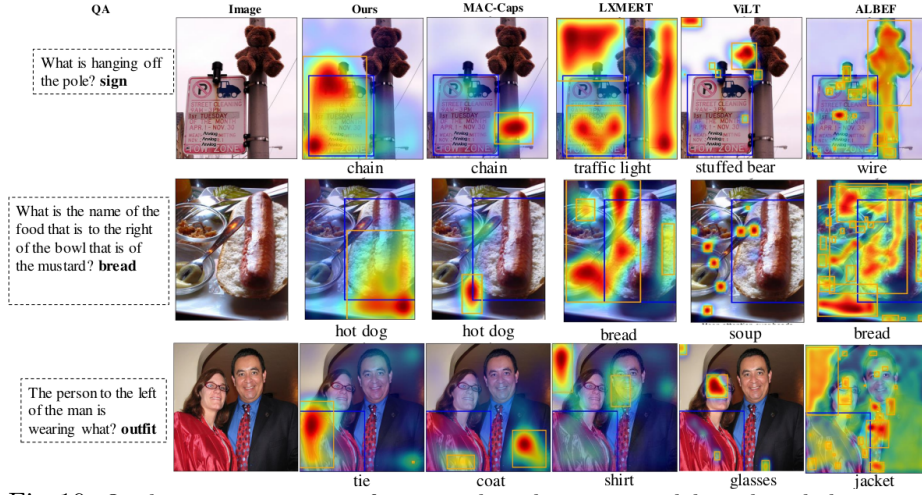


Fig. 10: Qualitative comparison for examples where our model predicted the wrong answer. The attention is over the correct image region.

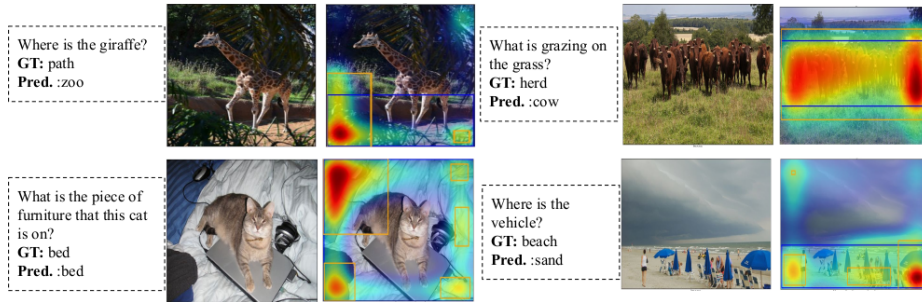


Fig. 11: Some failure cases for our system. Left two examples show the failure of grounding, right two examples are failure cases in terms of answer prediction. However, both the grounding output and the answers are plausible.

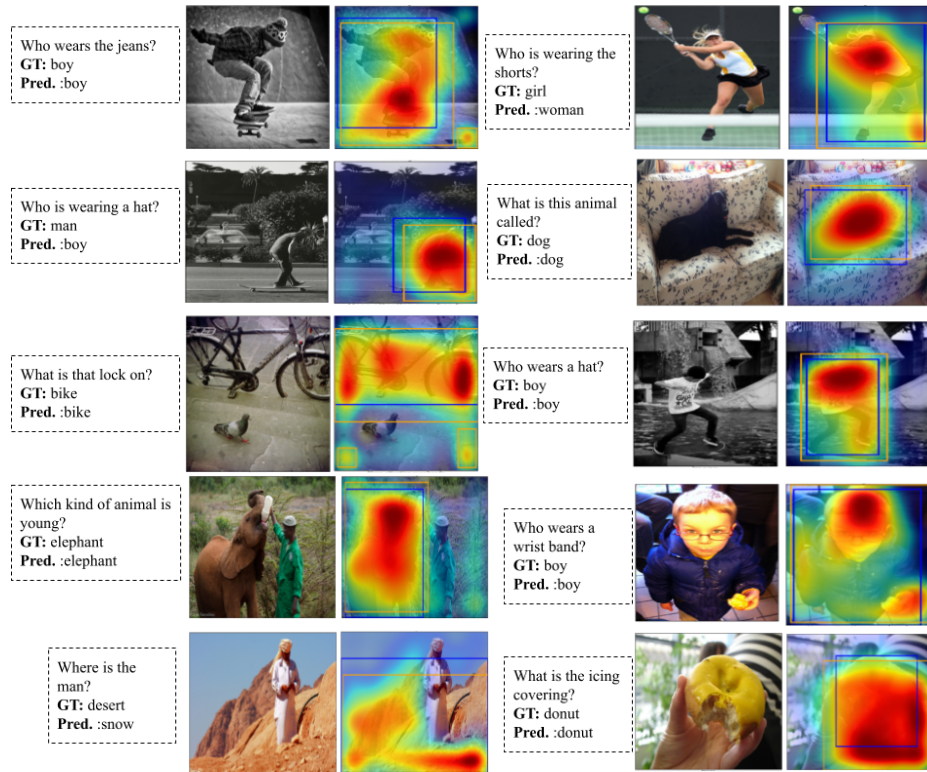


Fig. 12: More qualitative examples from our system.